RESEARCH ARTICLE

Mitochondria–Endoplasmic Reticulum Contact Sites Dynamics and Calcium Homeostasis Are Differentially Disrupted in *PINK1*-PD or *PRKN*-PD Neurons

Dajana Grossmann, PhD,[1] Nina Malburg,[1] Hannes Glaß, PhD,[1] Veronika Weeren,[1] Verena Sondermann, BSc,[1] Julia F. Pfeiffer, BSc,[1] Janine Petters, MSc,[1] Jan Lukas, PhD,[1,2] Philip Seibler, PhD,[3] Christine Klein, MD,[3] Anne Grünewald, PhD,[3,4] and Andreas Hermann, MD, PhD[1,2,5*]

[1]*Translational Neurodegeneration Section "Albrecht Kossel," Department of Neurology, University Medical Center Rostock, University of Rostock, Rostock, Germany*
[2]*Center for Transdisciplinary Neurosciences Rostock, University Medical Center Rostock, University of Rostock, Rostock, Germany*
[3]*Institute of Neurogenetics, University of Lübeck, Lübeck, Germany*
[4]*Luxembourg Centre for Systems Biomedicine, University of Luxembourg, Belvaux, Luxembourg*
[5]*Deutsches Zentrum für Neurodegenerative Erkrankungen Rostock/Greifswald, Rostock, Germany*

ABSTRACT: Background: It is generally believed that the pathogenesis of PINK1/parkin-related Parkinson's disease (PD) is due to a disturbance in mitochondrial quality control. However, recent studies have found that PINK1 and Parkin play a significant role in mitochondrial calcium homeostasis and are involved in the regulation of mitochondria–endoplasmic reticulum contact sites (MERCSs).

Objective: The aim of our study was to perform an in-depth analysis of the role of MERCSs and impaired calcium homeostasis in PINK1/Parkin-linked PD.

Methods: In our study, we used induced pluripotent stem cell–derived dopaminergic neurons from patients with PD with loss-of-function mutations in *PINK1* or *PRKN.* We employed a split-GFP-based contact site sensor in combination with the calcium-sensitive dye Rhod-2 AM and applied Airyscan live-cell super-resolution microscopy to determine how MERCSs are involved in the regulation of mitochondrial calcium homeostasis.

Results: Our results showed that thapsigargin-induced calcium stress leads to an increase of the abundance of narrow MERCSs in wild-type neurons. Intriguingly, calcium levels at the MERCSs remained stable, whereas the increased net calcium influx resulted in elevated mitochondrial calcium levels. However, *PINK1*-PD or *PRKN*-PD neurons showed an increased abundance of MERCSs at baseline, accompanied by an inability to further increase MERCSs upon thapsigargin-induced calcium stress. Consequently, calcium distribution at MERCSs and within mitochondria was disrupted.

Conclusions: Our results demonstrated how the endoplasmic reticulum and mitochondria work together to cope with calcium stress in wild-type neurons. In addition, our results suggests that *PRKN* deficiency affects the dynamics and composition of MERCSs differently from *PINK1* deficiency, resulting in differentially affected calcium homeostasis. © 2023 The Authors. *Movement Disorders* published by Wiley Periodicals LLC on behalf of International Parkinson and Movement Disorder Society.

Key Words: PINK1; Parkin; Parkinson´s disease; mitochondria–ER contact sites; calcium

***Correspondence to:** Prof. Dr. Andreas Hermann, Schilling Professor for Translational Neurodegeneration, Translational Neurodegeneration Section "Albrecht Kossel," Department of Neurology, University Medical Center Rostock, Gehlsheimer Straße 20, 18147 Rostock, Germany; E-mail: andreas.hermann@med.uni-rostock.de

Relevant conflicts of interest/financial disclosures: A.H. has received funding from the Hermann und Lilly Schilling-Stiftung für medizinische Forschung im Stifterverband.

Funding agencies: This work was supported by the Nachwuchsförderung der Deutschen Gesellschaft für Parkinson und Bewegungsstörungen e.V. (D.G.). A.H. was supported by the Hermann und Lilly Schilling-Stiftung für medizinische Forschung im Stifterverband. A.G. was supported by the Luxembourg National Research Fund (FNR) within the ATTRACT programme (Model-IPD, FNR9631103). A.G. was also supported by a donation from Le Foyer Assurances Luxembourg. C.K. and P.S. were supported by the German Research Foundation (FOR2488).

Received: 10 May 2023; **Accepted:** 16 June 2023

Published online 14 July 2023 in Wiley Online Library (wileyonlinelibrary.com). DOI: 10.1002/mds.29525

Introduction

The demise of dopaminergic neurons in the substantia nigra pars compacta of the midbrain is a pathological hallmark of Parkinson's disease (PD). Although the exact molecular mechanisms causing neurodegeneration in PD currently remain elusive, mitochondrial dysfunction has been established as a key aspect of the disease.[1,2] About 90% of patients with PD are affected by a sporadic form, which typically starts at the age of 65 years or older.[3] Familial cases are due to mutations in PD-linked genes, half of which encode for proteins involved in mitochondrial homeostasis and function. The most frequent recessive form of early-onset PD is caused by mutations in *PRKN*,[4,5] whereas mutations in *PINK1* account for the second most common form of early-onset PD.[6]

PRKN encodes the E3 ubiquitin ligase Parkin, which acts together with the mitochondrial kinase PINK1 to initiate the selective removal of damaged mitochondria by lysosomes.[7] However, the cellular functions of both PINK1 and Parkin go far beyond the regulation of mitophagy.

Connected to its involvement in mitochondrial quality control, PINK1 and Parkin have also been ascribed a role as regulator of mitochondria–endoplasmic reticulum (ER) contact sites (MERCSs).[8] MERCSs create a hub for phospholipid metabolism that is required to provide membranes for the formation of autophagosomes.[9,10] Moreover, when mitophagy is induced, MERCSs must be deconstructed to allow the degradation of liberated mitochondria.[11] This detethering of mitochondria from the ER is mediated via the PINK1/Parkin-dependent ubiquitination pathway and subsequent proteasomal degradation of various proteins that function at MERCSs, including MFN2, voltage-dependent anion channel (VDAC), or Miro1.[12-15]

The impact of PINK1 or Parkin pathogenic variants on the structure of MERCSs may also contribute to calcium dyshomeostasis. Different types of MERCS are defined by the cleft width between mitochondria and the ER membrane. Narrow MERCSs have been ascribed a role in the regulation of cellular calcium homeostasis[9,16] by creating microdomains for the transfer of calcium between both organelles via inositol-1,4,5-triphosphate (IP_3) receptors at the ER and VDAC at the outer mitochondrial membrane and the mitochondrial calcium uniporter at the inner mitochondrial membrane.[9,17-19] The maintenance of mitochondrial calcium levels is, among others, important for the enzymes of the tricarboxylic acid cycle, thereby modulating mitochondrial pyruvate and NAD^+ concentrations.[20,21]

To date, we do not understand exactly how MERCSs are dysregulated by the absence of PINK1 or Parkin. There have been conflicting reports about the effect of PINK1/Parkin-PD models on MERCSs, including reports of increased MERCSs and mitochondrial calcium,[22-24] but also others showing the opposite.[12,25,26] Although these differences might arise from different cell models or expression systems used, the differential contribution of narrow and wide MERCSs to the previously reported MERCS dysregulation was not systematically studied so far.

Furthermore, the mechanism by which MERCSs respond to calcium stress and how MERCSs coordinate the transfer of calcium ions from the ER to mitochondria remain enigmatic. In our study, using induced pluripotent stem cell (iPSC)-derived neurons, we showed that thapsigargin-induced calcium stress leads to a rapid increase in MERCS abundance to maintain stable calcium levels at each contact site, while enabling an increase in total mitochondrial calcium levels. iPSC-derived neurons with deleterious mutations in *PINK1* or *PRKN* showed an increase of total MERCSs already under baseline conditions, but also an alteration of the distribution of the calcium sensor Miro1 at different types of MERCS. We hypothesize that this disables *PINK1*- or *PRKN*-PD neurons to adapt the number of MERCSs under calcium stress, which presumably contributes to the dysregulation of mitochondrial calcium levels in these cells.

Subjects and Methods

Cell Culture

Generation and Characterization of iPSCs

For this study, we used iPSC lines of three healthy donors, two patients with PD with loss-of-function mutations in *PINK1* (c.1366C>T), and two patients with PD with loss-of-function mutations in *PRKN* (delEx1; c.823C>T), as described in Table 1. These mutations were previously shown to cause loss of PINK1[27] or Parkin, respectively.[28] All iPSC lines were previously published, except control_3 and *PINK1*_1. Control_3 was reprogrammed from fibroblasts using retrovirus, and *PINK1*_1 was reprogrammed using Sendai virus. The characterization was performed as described earlier.[29]

Generation of smNPC and Differentiation of Neurons

The described iPSC lines were used for further differentiation into small molecule–derived neuronal precursor cells (smNPCs) according to a previously published protocol.[34] The successful generation of smNPCs was judged based on cell morphology and on quantitative polymerase chain reaction for the following primers: 18S (5′–3′: CGTAGTTCCGACCATAAACGATGCC; 3′–5′: GTGGTGCCCTTCCGTCAATTCC), OCT4 (5′–3′: CTTCGCAAGCCCTCATTTCACCA; 3′–5′: GTC CGAGGATCAAACCAGCCC), NANOG (5′–3′: AGC AATGGTGTGACGCAGAAGGC; 3′–5′: TGGAAGG

TABLE 1 *Overview of iPSC lines used to differentiate into smNPCs*

ID of iPSC clone	Internal ID	Sex	Disease	Age at biopsy (y)	Mutation	Reference
2062-2	control_1	Male	Healthy	43	–	Peter et al[30]
GM23251-4	control_2	Female	Healthy	50	–	Petters et al[29]
D2-26	control_3	Female	Healthy	48	–	–
L3244	*PRKN*_1	Female	*PRKN*-PD	41	Compound heterozygous delEx1; c.823C>T [p.Arg275Trp]	Zanon et al[31]
SFC818-03-04	*PRKN*_2	Male	*PRKN*-PD	57	Compound heterozygous: delEx4; c.823C>T [p.Arg275Trp]	Trilck-Winkler et al[32]
SFC825-04-05	*PINK1*_1	Female	*PINK1*-PD	61	Homozygous: c.1366C>T [p.Gln456Ter]	–
SFC826-04-06	*PINK1*_2	Female	*PINK1*-PD	72	Homozygous: c.1366C>T [p.Gln456Ter]	Baud et al[33]

Abbreviations: iPSC, induced pluripotent stem cell; smNPC, small molecule–derived neuronal precursor cell; ID, identification number.

TTCCCAGTCGGGTTCA), AFP (5′–3′: AGCTTGGT GGTGGATGAAAC; 3′–5′: CCCTCTTCAGCAAA GCAGAC), T (5′–3′: ACCCAGTTCATAGCGGTGAC; 3′–5′: CAATTGTCATGGGATTGCAG), SOX17 (5′–3′: CCTGGGTTTTTGTTGTTGCT; 3′–5′: GAGGAA GCTGTTTTGGGACA), SOX2 (5′–3′: CAGCCCATG CACCGCTACGA; 3′–5′: TCGGACTTGACCACCGA ACCC), PAX6 (5′–3′: AGCACCAGTGTCTACCA ACC; 3′–5′: CGCTGTAGGTGTTTGTGAGG), HES5 (Qiagen: QT00202699), ASCL1 (5′–3′: GTCTCCCG GGGATTTTGTAT; 3′–5′: TCTCCATCTTGGCAGA GCTT), SOX1 (5′–3′: TGGGCTCTCTGGTGAAGT CGG; 3′–5′: GGCGCTAGATGTGCGTCAGG), PAX3 (5′–3′: CTGGAACATTTGCCCAGACT; 3′–5′: TAT CCAGGTGAAGGCGAAAC), HOXA2 (5′–3′: TTCA GCAAAATGCCCTCTCT; 3′–5′: TAGGCCAGCTCC ACAGTTCT), and HOXB2 (5′–3′: TTTAGCCGTTCG CTTAGAGG; 3′–5′: CGGATAGCTGGAGACAGG AG). The smNPCs were further used for differentiation into neuronal cultures, according to a previously published protocol.[34] The neuronal cultures were characterized by immunostaining with antibodies against MAP2 (1:1000; ab5392; Abcam) and TH (1:1000; T1299; Sigma-Aldrich). With the applied protocol, we obtained 70% to 80% neurons, of which 30% to 50% were TH positive. These proportions did not differ significantly between the lines.

Institutional Review Board Statement

The performed procedures were in accordance with the Declaration of Helsinki (World Medical Association, 1964) and approved by the Ethical Committee of the Technische Universität Dresden, Germany (EK 393122012 and EK 45022009) and the Universität Rostock (A2019-0134).

Informed Consent Statement

Written informed consent was obtained from all participants, including for publication of any research results.

Immunostainings and Microscopy

Neurons were fixed at day 23 or 24 in vitro with 4% paraformaldehyde, prewarmed to 37°C for 20 minutes, then permeabilized in 0.2% Triton X-100 for 10 minutes. Afterward, cells were washed three times in Tris-buffered saline containing 1% Tween 20 (in PBS) for 10 minutes and blocked in Pierce Protein-free blocking buffer (37572; Thermo Fisher) for 1 hour at room temperature. The following primary antibodies were diluted in Pierce Protein-free blocking buffer and incubated overnight at 4°C on a shaker: TOM20 (1:1000; sc-17764; Santa Cruz), KDEL (1:1000; MA5-34715; Invitrogen), Miro1 (1:500; HPA010687; Sigma), and HSP60 (1:1000; ab46798; Abcam). After three times washing in TBS-T for 10 minutes, secondary antibodies were diluted 1:10,000 in TBS-T and incubated for 1.5 hours at room temperature, on a shaker. After three times washing in TBS-T for 10 minutes, cells were mounted in DAPI Fluoromount-G mounting medium (0100-20; Southern Biotechnology). Images were acquired on a Zeiss inverted AxioObserver.Z1 microscope with LSM 900 module and high-resolution Airyscan 2 module, using a 63× 1.4 NA plan apochromat objective.

Data Analysis

Data acquired from microscopy were evaluated using macros in Fiji. Masks are depicted in the respective figures. Macros are included in the supplements. MERCSs were quantified based on TOM20 and KDEL signal overlap and depicted as area per nucleus. Colocalization of split-green fluorescent protein–based contact site sensor (SPLICS)-short or SPLICS-long with Miro1 was quantified based on signal overlap area per nucleus. All signals were quantified as area (pixel) per nucleus.

Super-Resolution Live-Cell Imaging

Super-resolution live-cell imaging was conducted on a Zeiss inverted AxioObserver.Z1 microscope with LSM 900 module and high-resolution Airyscan 2 module, using a 63× 1.4 NA plan apochromat objective and full environment control of CO_2, humidity, and temperature. Neurons were differentiated for 23–24 days according to a previously described protocol.[35]

Calcium Imaging

Neurons were transfected with FuseIT-DNA (60600; Beniag GmbH) with 0.5 µg SPLICS-short (164107; Addgene). Twenty-four hours posttransfection, neurons were stained with 100 nM MitoTracker Deep Red FM (8778; Cell Signaling) and 1 µM Rhod-2 AM (R1244; Invitrogen) for 30 minutes according to the manufacturer's instructions. Then the staining medium was removed, and the neurons were incubated in growth medium without staining for 4 hours before image acquisition. Image acquisition was done for 2 minutes in 10-second intervals, then DMSO or 1 µM thapsigargin (T9033; Sigma-Aldrich) treatments were applied, and image acquisition was continued for 2 minutes in 10-second intervals.

Data Analysis. Data acquired from live-cell imaging were evaluated using macros in Fiji. Masks are depicted in the respective figures. Macros are included in the Supporting Information.

Mitochondrial Membrane Potential

Neurons were stained with 100 nM MitoTracker Deep Red FM (8778; Cell Signaling) and 10 nM TMRE (T669; Invitrogen) for 30 minutes according to manufacturer's instructions for subsequent super-resolution live-cell imaging.

Data Analysis. Mean TMRE fluorescence intensity was measured within the MitoTracker mask area, using macros in Fiji. Masks are depicted in the respective figures. Macros are included in the Supporting Information.

Western Blot Analysis

Neuron cell pellets were lysed in radioimmunoprecipitation assay buffer (50 mM Tris–HCl, pH 7.4; 150 mM CaCl; 1% Triton X-100; 0.5% Na-deoxycholate; 0.1% sodium dodecyl sulfate [SDS]; cOmplete, EDTA-free protease inhibitor cocktail; 04693132001; Roche) for 30 minutes on ice. The lysate was incubated in Laemmli buffer for 6 minutes at 96°C. A total of 30 µg of total protein was loaded on 10% polyacrylamide-SDS gels for gel electrophoresis. Proteins were blotted on 0.2-µm nitrocellulose membrane (Trans-blot turbo transfer system RTA transfer kit, 1704270; BioRad), using a Trans-blot Turbo transfer system (22 V, 7 minutes; Bio-Rad). Total protein was stained with Ponceau S solution (SLCL2343; Sigma-Aldrich). The membrane was blocked in 5% skim milk (T145.3; in TBS; Roth) for 1 hour at room temperature. Afterward, primary antibodies against TOM20 (1:1000; sc17764; Santa Cruz); Calnexin (1:1000; ab22595; Abcam), or Miro1 (1:500; WH0055288M1; Sigma) were incubated in 5% skim milk (T145.3; in TBS; Roth) for 1 hour at room temperature. Secondary antibodies against mouse (1:5000; A16817; Invitrogen) or rabbit (1:5000; 611–144-122; Rockland) were incubated in TBS overnight at 4°C. Images were acquired on a Li-COR ODYSSEY XF analyzer. Signal intensities of protein bands were quantified using Fiji.

Statistics

For statistical analysis, we used GraphPad Prism 6.07. All data were tested for normal distribution by a D'Agostino-Pearson omnibus normality test. We used nonparametric tests as indicated in the figure legends. All experiments were independently repeated with at least three biological replicates, with one biological replicate defined as independent neuron differentiation. Cell lines with similar genetic backgrounds were pooled for analysis.

Results

Generation of Neuronal Cell Models

For this study, we reprogrammed human fibroblasts from a control and a PD patient with the homozygous c.1366C>T mutation in *PINK1*. The resulting generated iPSC lines were successfully characterized (Supporting Information Figs. S1. and S2.). A set of three control lines[29,30] (Supporting Information Fig. S1.) and two *PRKN*-PD[31,32] and two *PINK1*-PD[33] (Supporting Information Fig. S2.) iPSC lines were differentiated into smNPCs (for characterization see Supporting Information Fig. S3.). All experiments in this study were conducted with neurons differentiated from smNPCs,[34] after 2 weeks of maturation. We obtained 70% to 80% MAP2-positive neurons, of

which approximately 40% were TH positive in all used lines (Supporting Information Fig. S4.).

Analysis of MERCSs in PINK1-PD or PRKN-PD Neurons

Several previous studies have shown that PINK1 and Parkin are involved in the regulation of MERCSs by initiation of proteasomal degradation of MERCS-residing proteins. Consequently, deficiency of PINK1 or Parkin leads to decreased degradation of MERCS proteins, causing an increase or pathological stabilization of MERCSs.[8,12] Hence our first aim in this study was to assess the abundance of MERCSs in our patient-derived neurons. To this end, we quantified MERCSs by immunolabeling of TOM20 (for mitochondria) and KDEL (for the ER) and subsequent analysis of the colocalization of both proteins, indicated as signal overlap area (Fig. 1A). *PINK1*-PD neurons displayed a significant increase in the abundance of MERCSs per cell (Fig. 1B). Further analysis of the data showed that MERCS area per TOM20 was significantly increased only in *PINK1*-PD neurons (Fig. 1C), whereas MERCS area per KDEL was significantly increased only in *PRKN*-PD neurons (Fig. 1D). This observation was explained by an elevation of TOM20 signal area per cell in *PRKN*-PD neurons (Fig. 1E) and by elevated KDEL signal area per cell in *PINK1*-PD neurons (Fig. 1F). In addition, we quantified TOM20 and the ER protein Calnexin by Western blot analysis. Both proteins were not changed in PRKN-PD or PINK1-PD neurons, compared with controls (Fig. S6.A–C). Because MERCSs are strongly influenced by mitochondrial morphology and function,[36] and vice versa, we also determined mitochondrial membrane potential microscopically using MitoTracker and TMRE staining. Thereby, we observed that mitochondria from *PRKN*-PD and *PINK1*-PD neurons are slightly, but not statistically significant, depolarized compared with mitochondria from control neurons (Supporting Information Fig. S5.).

Our results suggest that alterations of the abundance of MERCSs might arise from different mechanisms in *PINK1*-PD or *PRKN*-PD neurons.

Structural Alterations of Specific Types of MERCS in PINK1-PD or PRKN-PD Neurons

Given the different functions and structures of MERCSs, we next wanted to investigate whether specific types of MERCS are differentially affected by loss of PINK1 or Parkin by using a molecular biology tool called SPLICS.[9] We transfected neuronal cultures with the SPLICS-short or the SPLICS-long construct for subsequent superresolution imaging, respectively (Fig. 2A). The GFP molecule is divided into two parts, encoded within the same vector, with one part being attached to the ER membrane and the other part being localized to the outer mitochondrial membrane. Only when both membranes are at a defined distance from each other do the two GFP parts connect and become fluorescent active. The distance between ER and mitochondria is defined by the length of a linker at the ER-split GFP part. Although the short linker of the construct (named SPLICS-short) allows the visualization of narrow MERCSs with a cleft width of ~15 nm, the SPLICS-long construct labels wide MERCSs with a cleft width of ~40 nm (Fig. 2B).[9] Indeed, quantification of the SPLICS-short and SPLICS-long signal area per cell showed an increased abundance of narrow and wide MERCSs in *PINK1*-PD or *PRKN*-PD neurons, compared with control neurons (Fig. 2C,D). These results suggest that the dysregulation of MERCSs in *PINK1*-PD or *PRKN*-PD is not restricted to a specific type of MERCS, but rather point to a systemic dysregulation of the MERCS architecture.

Having shown increased abundance of MERCSs, we were wondering whether these are associated to specific MERCS proteins. We thus focused our work on a protein, which putatively links PINK1 and Parkin with narrow and wide MERCSs. Miro1, which, albeit not responsible for the composition of MERCSs, plays a central role in MERCS stabilization and function[37,38] and is a target of PINK1/Parkin-mediated proteasomal degradation during the initiation phase of mitophagy.[15] Immunostaining of neurons transfected with SPLICS-short or SPLICS-long constructs with an antibody against Miro1 enabled us to quantify the distribution of Miro1 to specific types of MERCS (Fig. 2F). Notably, the overall level of Miro1 area per cell was comparable in control and mutant neurons (Fig. 2E). This observation was validated by Western blot analysis of Miro1 (Supporting Information Fig. S6.A,D). It is noteworthy that the majority of narrow and wide MERCSs did not colocalize with Miro1 (−Miro1) in all three genotypes (Fig. 2G,H), fitting with our previous findings.[39] We found an increase in narrow MERCSs associated with Miro1 (+Miro1) in *PINK1*-PD and *PRKN*-PD neurons (Fig. 2G), whereas only *PINK1*-PD neurons also showed an increase in narrow MERCSs, which do not colocalize with Miro1 (−Miro1) (Fig. 2G). In contrast, *PINK1*-PD or *PRKN*-PD mutations did not affect the colocalization of Miro1 at wide MERCSs (Fig. 2H).

Our data demonstrate differential alterations of Miro1 distribution, especially at narrow MERCSs in the absence of PINK1 or Parkin, besides a general increase in MERCS abundance.

Functional Alterations of MERCSs in PINK1-PD or PRKN-PD Neurons

Having found that *PINK1*-PD and *PRKN*-PD neurons show an increase of MERCSs and alterations of

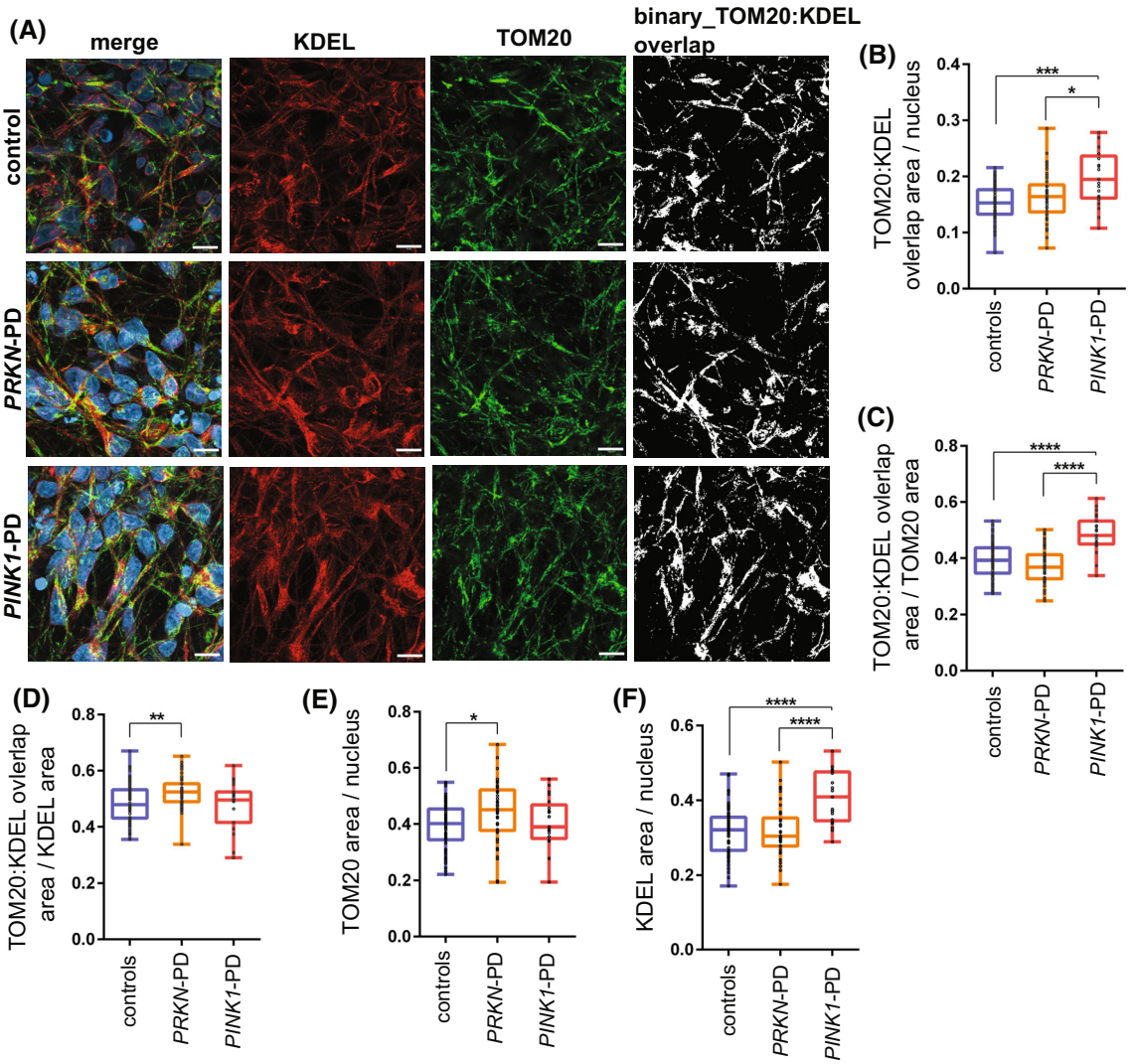

FIG. 1. Structural alterations of mitochondria–endoplasmic reticulum contact sites (MERCSs) in *PINK1*-PD or *PRKN*-PD neurons. (**A**) Neurons were fixed for immunolabeling with antibodies against TOM20 and KDEL for subsequent super-resolution microscopy. Scale bars, 10 μm. (**B**) MERCSs were quantified by colocalization area of TOM20 and KDEL, normalized per nucleus. (**C**) Colocalization area of TOM20 and KDEL (MERCSs) were normalized per TOM20 area (**D**) or per KDEL area. In addition, the (**E**) TOM20 and (**F**) KDEL signal area was quantified per nucleus. Data are indicated as median ± min/max (n = 3–6; n = 21–63). Significance was calculated by the Kruskal-Wallis test, with Dunn's multiple comparison post hoc test. $^{*}P < 0.05$, $^{**}P < 0.01$, $^{***}P < 0.001$, $^{****}P < 0.0001$.

Miro1 colocalization to narrow MERCSs, we next aimed to understand the functional consequences of this phenotype. Miro1 is an important regulator of mitochondrial calcium homeostasis by facilitating calcium exchange between the ER and mitochondria at MERCSs.[40,41,16] Particularly narrow MERCSs have been implicated in calcium homeostasis,[9,16] which was reported to be disturbed in *PINK1*-PD or *PRKN*-PD cells.[12,23] However, the exact molecular cause of this impairment remains elusive. We thus hypothesized that elevated MERCS numbers and increased abundance of Miro1 at narrow MERCSs contribute to calcium dyshomeostasis in *PINK1*-PD and *PRKN*-PD neurons.

For differential visualization of calcium, mitochondria, and MERCSs, we transfected neurons with SPLICS constructs and 24 hours posttransfection loaded with MitoTracker and the calcium indicator Rhod-2 AM (Fig. 3A,B). We used live-cell super-resolution microscopy to separately analyze calcium levels at different mitochondrial and MERCS subcompartments. We used the MitoTracker deep red signal to create a mask for mitochondria and the SPLICS signal to create a mask for MERCSs. The SPLICS mask subtracted from the mitochondrial mask creates a mask for a pure mitochondrial compartment ("mito"), which does not include SPLICS, whereas the SPLICS mask added to the mitochondrial mask creates the combined mask of the "mito+SPLICS" compartment. These masks were then used to assess Rhod-2 AM mean signal intensity in the respective compartments (Fig. 3C).

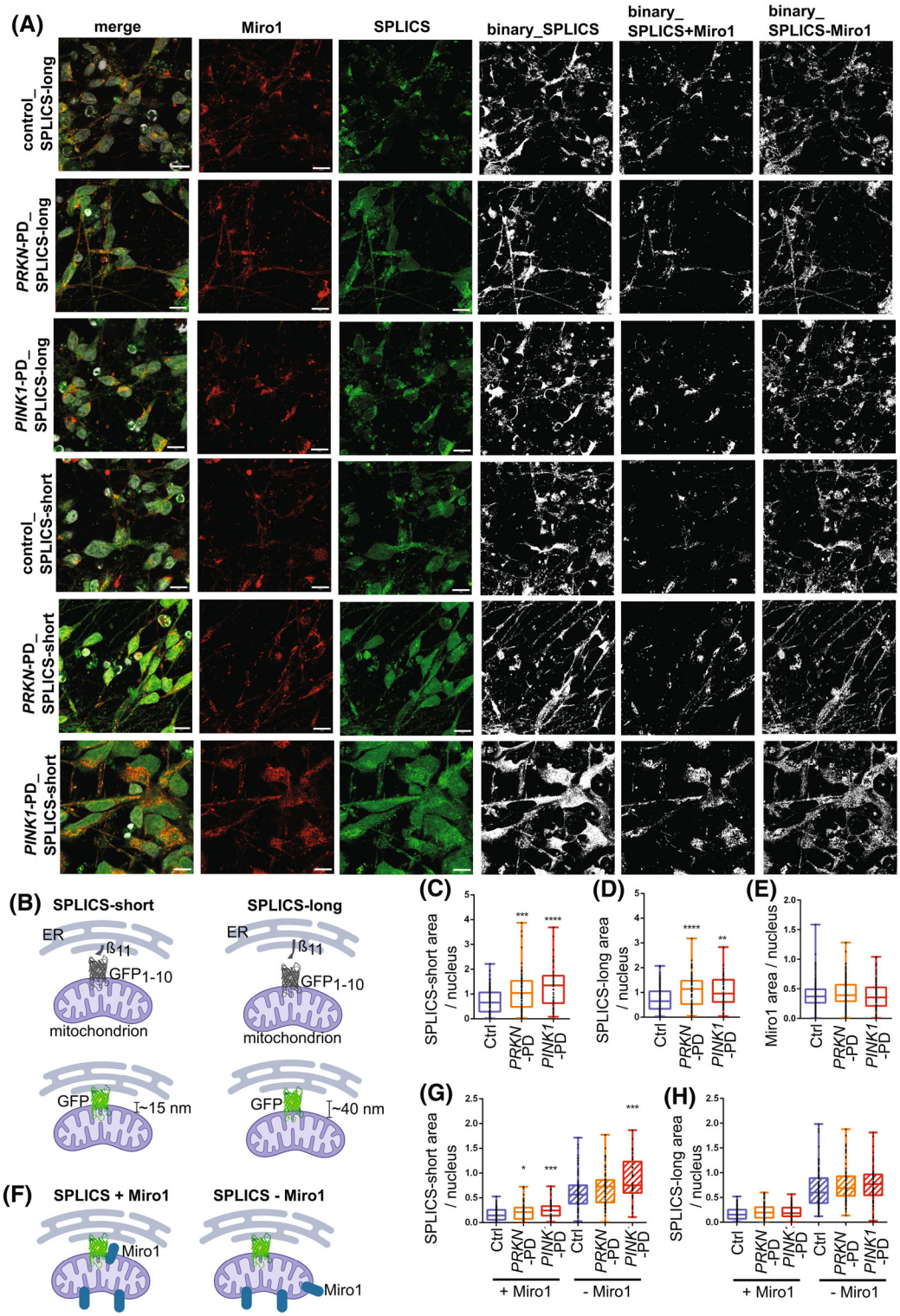

FIG. 2. Structural alterations of specific types of mitochondria–endoplasmic reticulum contact site (MERCS) in *PINK1*-PD or *PRKN*-PD neurons. (**A**) Neurons were transfected with SPLICS-short or SPLICS-long constructs. Twenty-four hours posttransfection, neurons were fixed for immunostaining with an antibody against Miro1. Images were acquired using super-resolution microscopy. Scale bars, 10 μm. (**B**) Schematic representation of SPLCIS-short and SPLICS-long markers. The image was generated using BioRender.com. Quantification of (**C**) SPLICS-short and (**D**) SPLICS-long signal area per nucleus. (**E**) Quantification of Miro1 signal area per nucleus. (**F**) Schematic representation of the analysis of SPLICSs colocalizing with Miro1 ("SPLICS + Miro1") or SPLICSs that are not colocalizing with Miro1 ("SPLICS –Miro1"). The image was generated using BioRender.com. Quantification of (**G**) SPLICS-short and (**H**) SPLICS-long area colocalizing with Miro1 (+ Miro1) or not colocalizing with Miro1 (− Miro1). Data are indicated as median ± min/max (n = 7–14; n = 50–106). Significance was calculated by the Kruskal-Wallis test, with Dunn's multiple comparison post hoc test. **P* < 0.05, ***P* < 0.01, ****P* < 0.001, *****P* < 0.0001.

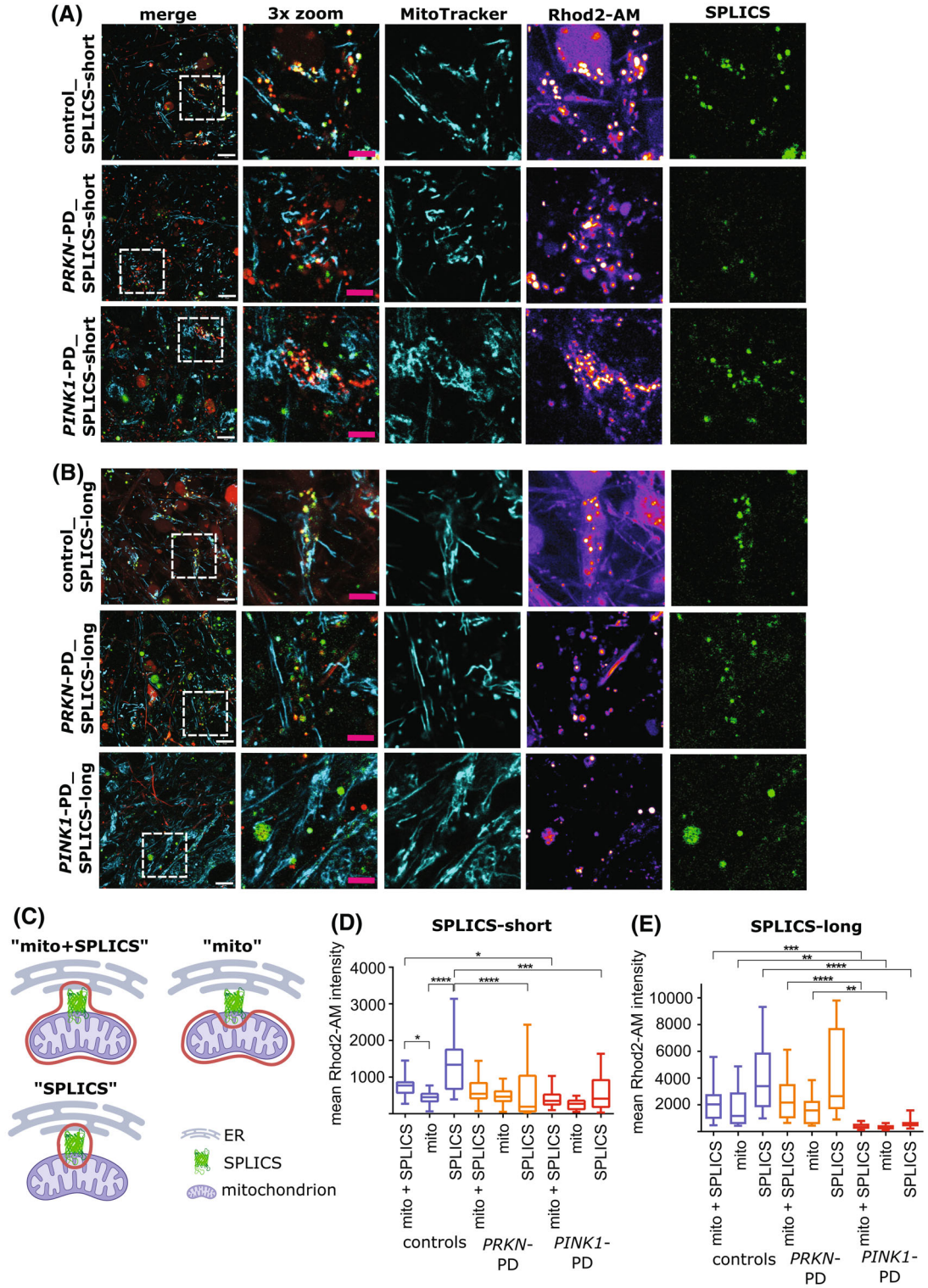

FIG. 3. Functional alterations of mitochondria–endoplasmic reticulum contact sites (MERCSs) in *PINK1*-PD or *PRKN*-PD neurons. Neurons were transfected with (**A**) SPLICS-short or (**B**) SPLICS-long constructs. Twenty-four hours posttransfection, neurons were stained with MitoTracker deep red and Rhod-2 AM for super-resolution live-cell imaging. White scale bars, 10 μm; red scale bars, 2 μm. (**C**) Schematic representation of the analysis of different compartments. Binary masks of the MitoTracker and SPLICS signals were created. Combination of the MitoTracker mask to the SPLICS mask results in the combined mitochondrial and SPLICS compartment ("mito+SPLICS"). Subtraction of the SPLICS mask from the MitoTracker mask results in the mask for the mitochondrial compartment ("mito"). The analyzed compartment is highlighted in red. The image was generated using BioRender.com. Quantification of calcium level, indicated by Rhod-2 AM mean fluorescence intensity in mito+SPLICS, mitochondrial (mito), or SPLICS compartments in neurons transfected with (**D**) SPLICS-short or (**E**) SPLICS-long. Data are indicated as median ± min/max (n = 3–7; n = 15–35). Significance was calculated by the Kruskal–Wallis test, with Dunn's multiple comparison post hoc test. *$P < 0.05$, **$P < 0.01$, ***$P < 0.001$, ****$P < 0.0001$.

In control cells, the calcium level of the combined mitochondria+SPLICS-short compartment ("mito +SPLICS") was indistinguishable from calcium levels at SPLICS-short ("SPLICS"), whereas the calcium levels at the purely mitochondrial compartment ("mito") were significantly lower compared with the "mito+SPLICS" and the "SPLICS" compartments. This observation suggests that calcium is not equally distributed in the mitochondrial compartment, but rather accumulates at narrow MERCSs under basal conditions in control neurons. Notably, there were no significant differences with respect to the calcium levels between any of the assessed compartments in *PRKN*-PD or *PINK1*-PD neurons (Fig. 3D). However, calcium levels at SPLICS-short ("SPLICS") were significantly reduced in *PRKN*-PD and *PINK1*-PD neurons compared with calcium at SPLICS-short in control neurons. In addition, the calcium level in the combined "mito+SPLICS-short" compartment was reduced in *PINK1*-PD neurons compared with controls (Fig. 3D).

When analyzing neurons transfected with SPLICS-long, we noticed that calcium levels were indistinguishable between mitochondria, including SPLICS-long ("mito+ SPLICS"), the pure mitochondrial compartment ("mito"), and at the SPLICS-long compartment ("SPLICS") within each genotype. Interestingly, however, calcium levels were decreased in all compartments only in the case of *PINK1*-PD neurons, both if compared with control and *PRKN*-PD neurons (Fig. 3E).

In summary, our analysis supports the paradigm that narrow MERCSs (labeled by SPLICS-short constructs) are mainly responsible for calcium exchange between the ER and mitochondria.[9,16] Furthermore, our results show impaired calcium homeostasis in *PRKN*-PD and *PINK1*-PD neurons.

Dynamic Modulation of MERCSs and Calcium Transfer Is Impaired in PINK1-PD or PRKN-PD Neurons

Based on our results of alterations of local calcium levels at narrow MERCSs in *PINK1*-PD or *PRKN*-PD neurons, we were interested in further analyzing the calcium dynamics at narrow MERCSs under calcium stress. For this purpose, neurons were transfected with SPLICS-short constructs and 24 hours posttransfection stained with MitoTracker deep red and Rhod-2 AM for subsequent dynamic super-resolution live-cell microscopy (Fig. 4A). First, we recorded 2 minutes of baseline calcium dynamics; then we applied 1 μM thapsigargin and continued recording for another 2 minutes (Fig. 4B). Thapsigargin is an inhibitor of the sarcoplasmic/ER calcium ATPase (SERCA) pumps, preventing calcium uptake by the ER and hence forcing calcium uptake by the mitochondria via MERCSs.[42]

Calcium levels were expressed as a fold change of mean Rhod-2 AM intensity normalized to the mean baseline signal before the thapsigargin application. We analyzed the same compartments as in Figure 3. When analyzing the total mitochondria, including SPLICS ("mito+SPLICS"), control and *PRKN*-PD neurons showed increased calcium levels after thapsigargin application, compared with the baseline levels, whereas *PINK1*-PD neurons showed no change of calcium levels (Fig. 4C).

Analysis of the mitochondrial compartment ("mito") indicated a thapsigargin-induced increase of mitochondrial calcium levels in control neurons. By contrast, in *PRKN*-PD or *PINK1*-PD neurons, no change was observed (Fig. 4D). When analyzing the local calcium levels at narrow MERCSs specifically, we found no thapsigargin-induced increase in control neurons. In contrast, *PRKN*-PD neurons showed significantly increased local calcium levels at MERCSs after thapsigargin application. However, *PINK1*-PD neurons showed no change of calcium levels at MERCSs (Fig. 4E).

Intriguingly, quantification of the SPLICS-short signal area demonstrated that control neurons react with a rapid increase of narrow MERCSs within approximately 1 minute after thapsigargin application, an effect that was not observed in *PRKN*-PD or *PINK1*-PD neurons (Fig. 4F).

Taken together, our results suggest that, in wild-type conditions, calcium levels are increased at narrow MERCSs, thereby facilitating calcium transfer between ER and mitochondria. *PINK1*-PD neurons show a strong, whereas *PRKN*-PD neurons a modest, reduction of calcium levels at MERCSs already under basal conditions. When mitochondria are additionally forced to take up more calcium because of thapsigargin treatment, the physiological response is to form more MERCSs to ensure increased net calcium uptake while maintaining stable calcium levels at each individual contact site. In *PINK1*-PD or *PRKN*-PD neurons, which already showed increased MERCSs under basal conditions, this mechanism appears to be exhausted. Whereas in the case of SERCA inhibition, *PRKN*-PD neurons were able to react by increasing the calcium flow at narrow MERCSs, *PINK1*-PD neurons completely failed to react, suggesting a differential vulnerability against calcium stress.

Discussion

The two PD-associated proteins PINK1 and Parkin are known mainly for their role in the mitophagy signalling pathway.[43] However, an increasing number of studies identified other functions of PINK1 and Parkin in recent years, leading to a broad spectrum of diverse phenotypes, including, but not limited to, disturbed

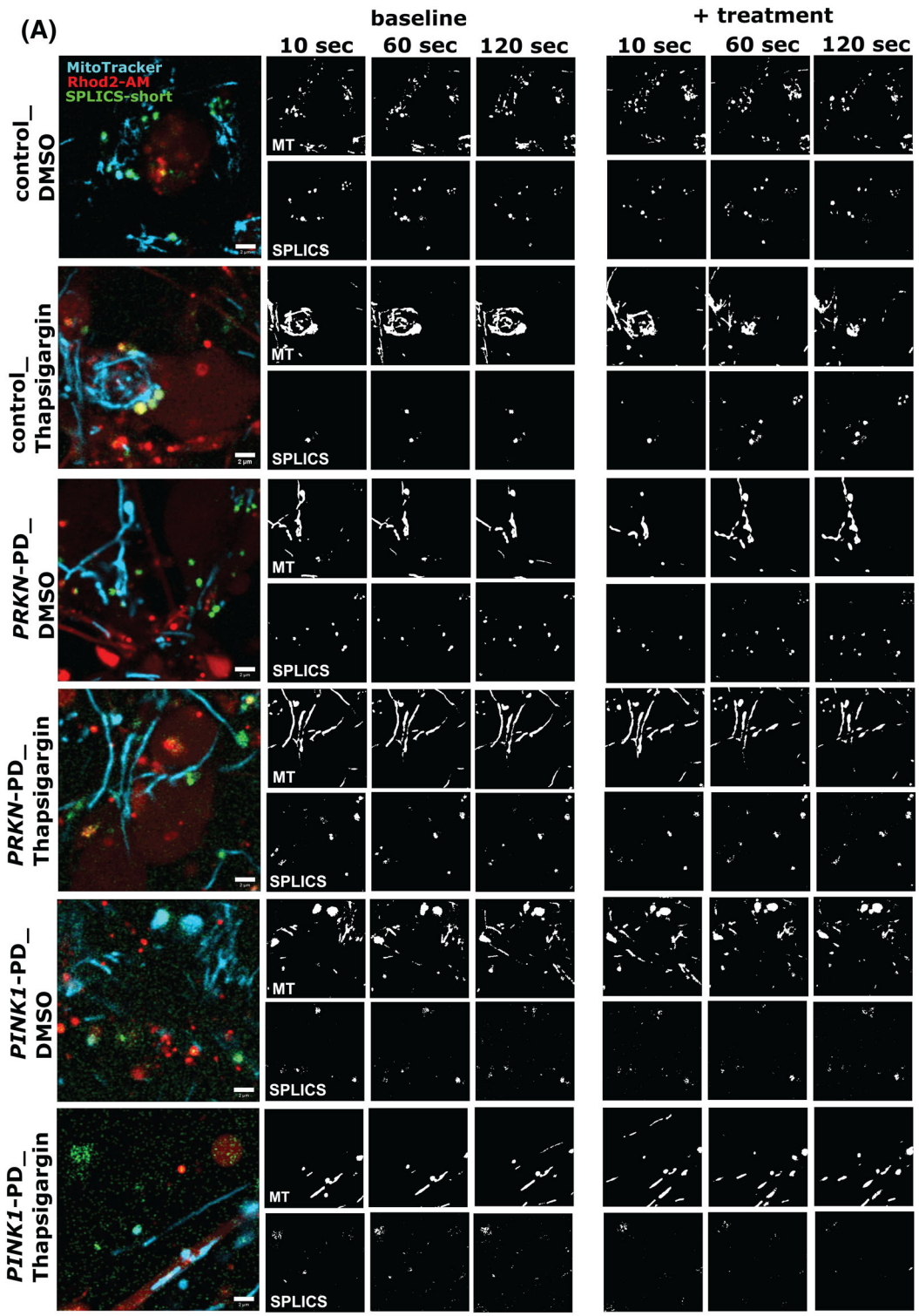

FIG. 4. Dynamic modulation of mitochondria–endoplasmic reticulum contact sites (MERCSs) and mitochondrial calcium transients is impaired in *PINK1*-PD or *PRKN*-PD neurons. (**A**) Neurons were transfected with SPLICS-short constructs. Twenty-four hours posttransfection, neurons were stained with MitoTracker deep red and Rhod-2 AM for super-resolution live-cell time-lapse imaging. Neurons were imaged with a 10-seconds interval for 2 minutes without treatment (baseline). Then, either DMSO or 1 µM thapsigargin treatments were applied, and image acquisition was continued for another 2 minutes, with 10-second intervals (+ treatment). Scale bars, 2 µm. (**B**) Schematic overview of the experimental setup. The image was generated with BioRender.com. From these time-lapse images, we quantified (**C**) calcium levels of the combined mitochondria and SPLICS-short compartment (mito+SPLICS), (**D**) calcium levels of the mitochondrial compartment (mito), and (**E**) calcium levels at the SPLICS-short compartment. Relative calcium levels were assessed based on the mean fluorescence intensity of the Rhod-2 AM signal. The fluorescence intensity of each time point was normalized to the mean fluorescence intensity of the 2-minute baseline recording. (**F**) SPLICS area was quantified, and the area of each time point was normalized to the mean area of the 2-minute baseline recording. Data are indicated as mean ± SEM (n = 3–5). Significance was calculated by two-Way ANOVA, with Sidak's multiple comparison post hoc test. $^{*}P \leq 0.01$, $^{**}P \leq 0.001$, $^{***}P \leq 0.0001$.

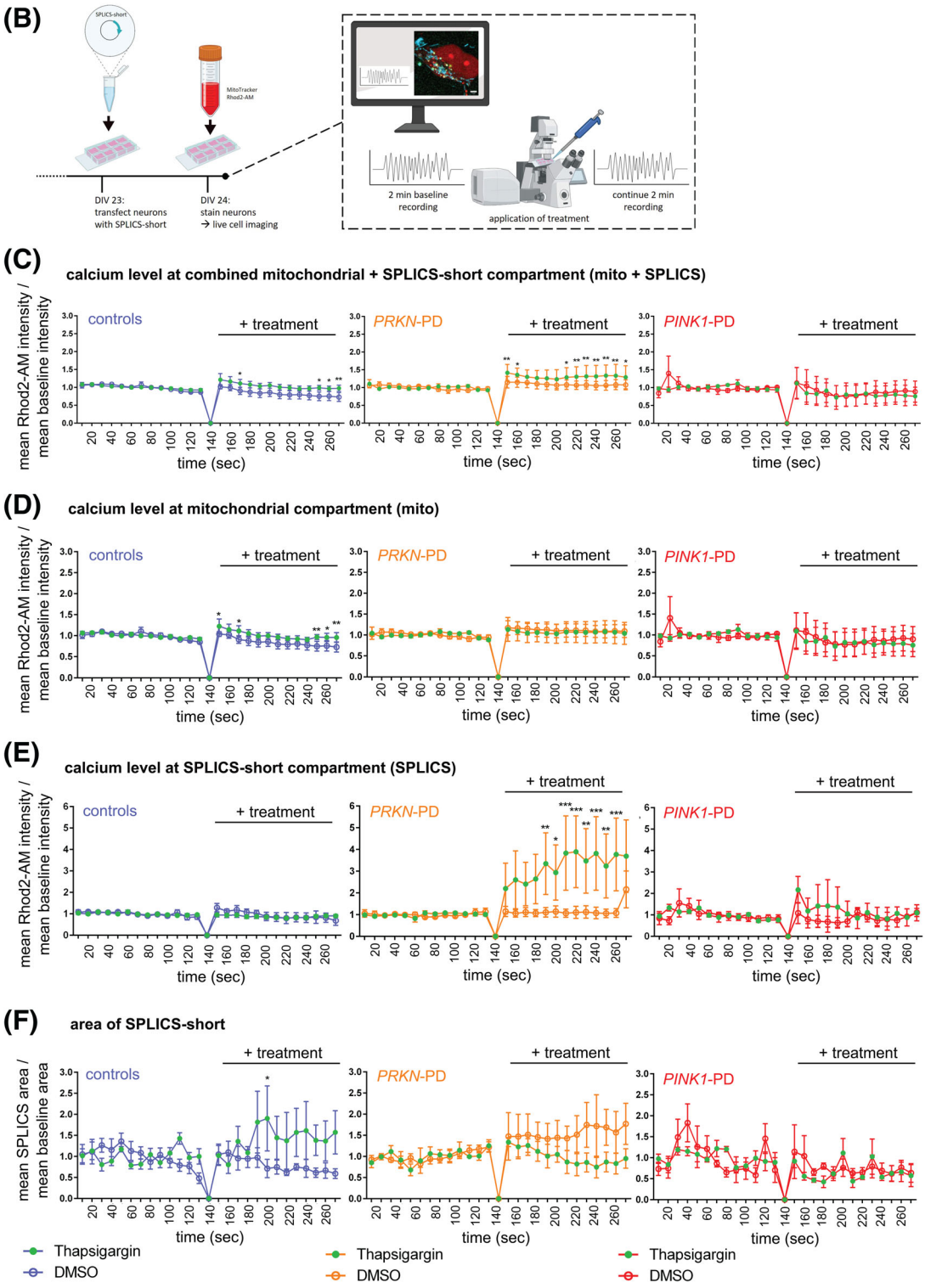

FIG 4 (Continued)

calcium homeostasis, mitochondrial dysfunction, and dysregulation of MERCSs.[44] In fact, we were able to show an increased abundance of MERCSs in *PINK1*-PD or *PRKN*-PD neurons, as previously described by other groups.[22-24] We were able to show that both types of MERCS, narrow and wide, are likewise increased in *PINK1*-PD or *PRKN*-PD neurons using previously described SPLICS constructs[9] in combination with super-resolution Airyscan microscopy. Hence we speculate that the increase in MERCSs is not only

caused by impaired protein degradation at MERCSs via disruption of the PINK1/Parkin pathway, but also by differential effects, which might be independent of the canonical PINK1/Parkin pathway.

Our results further support that narrow MERCSs (visualized by SPLICS-short) in particular were associated with the regulation of calcium homeostasis by facilitating the calcium transfer between the ER and mitochondria.[9,16]

When analyzing the resting levels of calcium in mitochondrial subcompartments, we first realized that calcium levels were significantly lower in the pure mitochondrial compartment, compared with calcium levels at narrow MERCSs in control neurons. The surprisingly low calcium levels in the mitochondrial compartments observed in this study might be explained by the fact that we used super-resolution live-cell imaging to separately analyze the mitochondrial and MERCS compartments. Conventional microscopy usually shows mitochondria and MERCSs as a combined compartment because of limited resolution. However, our analysis shows that, under physiological conditions, calcium levels of the combined "mito+SPLICS" compartment were comparable with the levels in the "SPLICS" compartment, suggesting that the main mitochondrial calcium load arises from high calcium levels at MERCSs in wild-type cells. By contrast, in *PINK1*-PD and *PRKN*-PD neurons, this difference in calcium levels between compartments was no longer observed, suggesting that calcium transfer at narrow MERCSs might be disrupted in the absence of PINK1 or Parkin.

We aimed to further analyze the response upon forced calcium entry into the mitochondria using thapsigargin. Our results suggest that wild-type cells cope with thapsigargin-induced calcium stress by increasing the abundance of narrow MERCSs, to open more gates to allow a net increase of calcium in the matrix, while keeping the calcium levels at narrow MERCSs constant. A previous study showed that MERCSs are increased in response to ER stress induced by 4 hours of tunicamycin treatment in wild-type HeLa cells and mouse embryonic fibroblasts.[45] Furthermore, an increase of SPLICS-short area was previously observed in HeLa cells after 24 hours of thapsigargin-induced ER stess.[9] In both studies, an adaption of MERCS abundance was induced by several hours of ER stress. In contrast, the area of MERCSs was increased much quicker in our setup of acute thapsigargin-induced calcium stress. Based on our data, we suggest a mechanism of how the ER and mitochondria work together to orchestrate cellular calcium homeostasis.

This fine-tuned balance between MERCS dynamics and calcium transfer appears to be disturbed in *PRKN*-PD neurons in a different manner than in *PINK1*-PD neurons: in *PRKN*-PD neurons the number of narrow MERCSs is increased already under basal conditions and cannot be further enhanced by calcium stress. Consequently, calcium levels were strongly elevated specifically at narrow MERCSs under thapsigargin treatment, whereas calcium levels were not increased in the mitochondrial compartment, indicating a blockage of calcium uptake.

In *PINK1*-PD neurons, the situation is different: although these cells also show an increase of narrow MERCSs at baseline conditions, they lack the ability to react to thapsigargin-induced calcium stress at all, either by elevating the number of MERCSs or by changing local calcium levels. *PINK1*-PD neurons show an increase of narrow MERCSs that are associated with Miro1. At the same time, they harbor more narrow MERCSs, which are not colocalizing with Miro1. Due to its functions as a calcium sensor,[40,46] as well as interactor and regulator of the mitochondrial calcium uniporter,[47] Miro1 plays a crucial role in the calcium uptake capacity of mitochondria.[40,47,48] Therefore, an increased proportion of MERCSs lacking Miro1 could hinder sensing of local calcium, as well as calcium uptake. Another aspect is that *PINK1*-PD neurons do not respond to thapsigargin, neither with an increase in mitochondrial calcium levels nor with a change in MERCSs. By inhibiting SERCA pumps, thapsigargin leads to calcium depletion from the ER, forcing mitochondria to take up calcium.[42,49] The lack of a mitochondrial response to thapsigargin despite the general increase of MERCSs thus suggests a calcium deficiency in the ER even before the thapsigargin treatment. Nevertheless, further studies with additional calcium modulators beyond thapsigargin will be needed to uncover the fundamental problem behind impaired calcium homeostasis in PINK1-PD and PRKN-PD neurons.

Although most research has focused on the impact of disrupted MERCSs on mitochondria, the effect on the ER is largely unexplored. It was recently proposed that PINK1 is associated with the ER proteostasis machinery, likely via MERCSs rather than via direct localization at the ER.[50] Interestingly, induction of proteotoxic ER stress via tunicamycin for 4 hours specifically enhanced the abundance of SPLICS-short in HeLa cells.[9] Furthermore, calcium depletion from the ER by a 24-hour application of thapsigargin was shown to increase MERCSs but also to cause secretion of proteins from the ER that specifically contain the ER retention signal, ie, KDEL, leading to an upregulation of KDEL receptors at the Golgi to counteract the secretion of ER proteins.[51] Compensatory effects such as this might explain our observation of increased KDEL signal in immunostainings in *PINK1*-PD neurons, whereas Western blot analysis did not show differences of the ER chaperone Calnexin. The paradigms in these studies most likely assessed completely different cellular

mechanisms than the acute calcium stress used in our approach, which was meant to measure immediate cellular reactions and is most likely too short to induce measurable ER stress. Further research will thus be necessary to elucidate the consequence of impaired MERCSs on the function of the ER, and vice versa, and the role of PINK1 and Parkin in this context.

Reviewing the literature on different models of PINK1 or Parkin, it is striking to note that calcium phenotypes and the mechanisms regulating MERCS dynamics appear to be highly complex and currently remain underexplored. Overexpression of wild-type *PRKN* in HeLa cells led to an increase of MERCSs and consequently increased mitochondrial calcium levels,[25] a phenotype that was later linked to an increase in SPLICS-short and a concomitant decrease in SPLICS-long.[9]

However, an increase in MERCSs was also observed as a result of PINK1 or Parkin loss of function in different models, eg, in PINK1- or Parkin-mutant flies or fibroblasts from patients with PD with homozygous mutations in *PINK1* or *PRKN*.[22-24]

Finally, it was also observed that reduced levels of *PINK1* or *PRKN* can have the opposite effect: ie, a reduction in MERCS abundance accompanied by lower mitochondrial calcium levels. This was the case in M17 cells with short hairpin RNA–mediated knockdown of *PINK1*,[26] in MEFs with RNA interference of *PRKN*,[12] or in SH-SY5Y cells with small interfering RNA knockdown of *PRKN*.[25] These might hint at differential effects depending on the cellular model system used or the degree of knockdown of the respective proteins.

In summary, we propose different mechanisms for impaired calcium homeostasis in *PINK1*- and *PRKN*-PD patient-derived neurons. In *PRKN*-PD neurons, we observed an upregulation of narrow and wide MERCSs, as well as an increased proportion of narrow MERCSs associated with Miro1. Calcium stress was not inducing a further elevation of narrow MERCSs but caused an increase of local calcium levels at narrow MERCSs, whereas the calcium influx into the mitochondria appears to be hampered. In *PINK1*-PD neurons, increased MERCSs also include an increase of narrow and wide MERCSs. In contrast with *PRKN*-PD neurons, *PINK1*-PD neurons showed increased proportions of narrow MERCSs colocalizing with Miro1, but also without Miro1. It is worth noting that overexpression of wild-type *Drosophila Miro* was shown to mimic the *PINK1* loss-of-function effect in a *Drosophila* PD model,[23] supporting our hypothesis of an involvement of Miro1 in the dysregulation of calcium homeostasis at narrow MERCSs in *PINK1*-PD neurons.

Upon thapsigargin-induced calcium stress, PINK1-PD neurons did not react at all, neither by an increase in the amount of narrow MERCSs nor by elevation of calcium levels at MERCSs or in the mitochondria. These results might hint toward a calcium deficiency not only of the mitochondria but also of the ER.

Collectively, our results support the conclusion that *PRKN* deficiency affects the dynamics and composition of MERCSs differently from *PINK1* deficiency, resulting in differentially affected calcium homeostasis. ■

Acknowledgments: The super-resolution imaging was performed at an LSM900 Airyscan (INST 264/175-1 FUGG). Open Access funding enabled and organized by Projekt DEAL.

Data Availability Statement

Data is available upon request.

References

1. Grünewald A, Kumar KR, Sue CM. New insights into the complex role of mitochondria in Parkinson's disease. Prog Neurobiol [Internet] 2019;177:73–93. Available from: https://linkinghub.elsevier.com/retrieve/pii/S0301008218300650
2. Rakovic A, Grünewald A, Kottwitz J, Brüggemann N, Pramstaller PP, Lohmann K, et al. Mutations in PINK1 and parkin impair ubiquitination of Mitofusins in human fibroblasts. PLoS One [Internet] 2011;6(3):e16746. Available from: http://www.ncbi.nlm.nih.gov/pubmed/21408142
3. Thomas B, Beal MF. Parkinson's disease. Hum Mol Genet [Internet] 2007;16:R183–R194. Available from: http://www.ncbi.nlm.nih.gov/pubmed/17911161
4. Kitada T, Asakawa S, Hattori N, Matsumine H, Yamamura Y, Minoshima S, et al. Mutations in the parkin gene cause autosomal recessive juvenile parkinsonism. Nature [Internet] 1998;392(6676):605–608. Available from: http://www.nature.com/articles/33416
5. Lücking CB, Dürr A, Bonifati V, Vaughan J, De Michele G, Gasser T, et al. Association between early-onset Parkinson's disease and mutations in the parkin gene. N Engl J Med [Internet] 2000;342(21):1560–1567. Available from:. https://doi.org/10.1056/NEJM200005253422103
6. Valente EM, Abou-Sleiman PM, Caputo V, Muqit MMK, Harvey K, Gispert S, et al. Hereditary early-onset Parkinson's disease caused by mutations in PINK1. Science [Internet] 2004;304(5674):1158–1160. Available from: http://www.ncbi.nlm.nih.gov/pubmed/15087508
7. Narendra D, Tanaka A, Suen D-F, Youle RJ. Parkin is recruited selectively to impaired mitochondria and promotes their autophagy. J Cell Biol [Internet] 2008;183(5):795–803. Available from: https://rupress.org/jcb/article/183/5/795/35265/Parkin-is-recruited-selectively-to-impaired
8. Valadas JS, Esposito G, Vandekerkhove D, Miskiewicz K, Deaulmerie L, Raitano S, et al. ER lipid defects in Neuropeptidergic neurons impair sleep patterns in Parkinson's disease. Neuron [Internet] 2018;98(6):1155–1169.e6. Available from: http://www.ncbi.nlm.nih.gov/pubmed/29887339
9. Cieri D, Vicario M, Giacomello M, Vallese F, Filadi R, Wagner T, et al. SPLICS: a split green fluorescent protein-based contact site sensor for narrow and wide heterotypic organelle juxtaposition. Cell Death Differ [Internet] 2018;25(6):1131–1145. Available from: http://www.nature.com/articles/s41418-017-0033-z
10. Hamasaki M, Furuta N, Matsuda A, Nezu A, Yamamoto A, Fujita N, et al. Autophagosomes form at ER-mitochondria contact sites. Nature [Internet] 2013;495(7441):389–393. Available from: http://www.ncbi.nlm.nih.gov/pubmed/23455425
11. McLelland G-L, Goiran T, Yi W, Dorval G, Chen CX, Lauinger ND, et al. Mfn2 ubiquitination by PINK1/parkin gates the p97-dependent release of ER from mitochondria to drive mitophagy. Elife [Internet] 2018;7:e32866. Available from: http://www.ncbi.nlm.nih.gov/pubmed/29676259

12. Basso V, Marchesan E, Peggion C, Chakraborty J, von Stockum S, Giacomello M, et al. Regulation of ER-mitochondria contacts by parkin via Mfn2. Pharmacol Res [Internet] 2018;138:43–56. Available from: http://www.ncbi.nlm.nih.gov/pubmed/30219582
13. Sun Y, Vashisht AA, Tchieu J, Wohlschlegel JA, Dreier L. Voltage-dependent anion channels (VDACs) recruit parkin to defective mitochondria to promote mitochondrial autophagy. J Biol Chem [Internet] 2012 Nov 23;287(48):40652–40660. Available from: http://www.ncbi.nlm.nih.gov/pubmed/23060438
14. Birsa N, Norkett R, Wauer T, Mevissen TET, Wu HC, Foltynie T, et al. Lysine 27 ubiquitination of the mitochondrial transport protein miro is dependent on serine 65 of the parkin ubiquitin ligase. J Biol Chem 2014;289(21):14569–14582.
15. Wang X, Winter D, Ashrafi G, Schlehe J, Wong YL, Selkoe D, et al. PINK1 and parkin target miro for phosphorylation and degradation to arrest mitochondrial motility. Cell [Internet] 2011;147(4):893–906. Available from:. https://doi.org/10.1016/j.cell.2011.10.018
16. Giacomello M, Pellegrini L. The coming of age of the mitochondria-ER contact: a matter of thickness. Cell Death Differ 2016;23(9):1417–1427.
17. Szabadkai G, Bianchi K, Várnai P, De Stefani D, Wieckowski MR, Cavagna D, et al. Chaperone-mediated coupling of endoplasmic reticulum and mitochondrial Ca2+ channels. J Cell Biol [Internet] 2006;175(6):901–911. Available from: http://www.ncbi.nlm.nih.gov/pubmed/17178908
18. Csordás G, Renken C, Várnai P, Walter L, Weaver D, Buttle KF, et al. Structural and functional features and significance of the physical linkage between ER and mitochondria. J Cell Biol [Internet] 2006;174(7):915–921. Available from: http://www.ncbi.nlm.nih.gov/pubmed/16982799
19. Csordás G, Várnai P, Golenár T, Roy S, Purkins G, Schneider TG, et al. Imaging interorganelle contacts and local calcium dynamics at the ER-mitochondrial interface. Mol Cell [Internet] 2010;39(1):121–132. Available from: http://www.ncbi.nlm.nih.gov/pubmed/20603080
20. Gherardi G, Monticelli H, Rizzuto R, Mammucari C. The mitochondrial Ca2+ uptake and the fine-tuning of aerobic metabolism. Front Physiol [Internet] 2020;11:554904. Available from: http://www.ncbi.nlm.nih.gov/pubmed/33117189
21. Marcu R, Wiczer BM, Neeley CK, Hawkins BJ. Mitochondrial matrix Ca^{2+} accumulation regulates cytosolic NAD^{+}/NADH metabolism, protein acetylation, and sirtuin expression. Mol Cell Biol [Internet] 2014;34(15):2890–2902. Available from: http://www.ncbi.nlm.nih.gov/pubmed/24865966
22. Celardo I, Costa AC, Lehmann S, Jones C, Wood N, Mencacci NE, et al. Mitofusin-mediated ER stress triggers neurodegeneration in pink1/parkin models of Parkinson's disease. Cell Death Dis [Internet] 2016;7(6):e2271. Available from: http://www.nature.com/articles/cddis2016173
23. Lee K-S, Huh S, Lee S, Wu Z, Kim A-K, Kang H-Y, et al. Altered ER-mitochondria contact impacts mitochondria calcium homeostasis and contributes to neurodegeneration in vivo in disease models. Proc Natl Acad Sci U S A [Internet] 2018;115(38):E8844–E8853. Available from: http://www.ncbi.nlm.nih.gov/pubmed/30185553
24. Gautier CA, Erpapazoglou Z, Mouton-Liger F, Muriel MP, Cormier F, Bigou S, et al. The endoplasmic reticulum-mitochondria interface is perturbed in PARK2 knockout mice and patients with PARK2 mutations. Hum Mol Genet [Internet] 2016;25(14):2972–2984. Available from: https://academic.oup.com/hmg/article-lookup/doi/10.1093/hmg/ddw148
25. Calì T, Ottolini D, Negro A, Brini M. Enhanced parkin levels favor ER-mitochondria crosstalk and guarantee Ca(2+) transfer to sustain cell bioenergetics. Biochim Biophys Acta [Internet] 2013;1832(4):495–508. Available from: http://www.ncbi.nlm.nih.gov/pubmed/23313576
26. Parrado-Fernández C, Schreiner B, Ankarcrona M, Conti MM, Cookson MR, Kivipelto M, et al. Reduction of PINK1 or DJ-1 impair mitochondrial motility in neurites and alter ER-mitochondria contacts. J Cell Mol Med [Internet] 2018;22(11):5439–5449. Available from: https://onlinelibrary.wiley.com/doi/10.1111/jcmm.13815
27. Grünewald A, Breedveld GJ, Lohmann-Hedrich K, Rohé CF, König IR, Hagenah J, et al. Biological effects of the PINK1 c.1366C>T mutation: implications in Parkinson disease pathogenesis. Neurogenetics [Internet] 2007;8(2):103–109. Available from: http://www.ncbi.nlm.nih.gov/pubmed/17219214
28. Wasner K, Smajic S, Ghelfi J, Delcambre S, Prada-Medina CA, Knappe E, et al. Parkin deficiency impairs mitochondrial DNA dynamics and propagates inflammation. Mov Disord [Internet] 2022;37(7):1405–1415. Available from: http://www.ncbi.nlm.nih.gov/pubmed/35460111
29. Petters J, Völkner C, Krohn S, Murua Escobar H, Bullerdiek J, Reuner U, et al. Generation of two induced pluripotent stem cell lines from a female adult homozygous for the Wilson disease associated ATP7B variant p.H1069Q (AKOSi008-a) and a healthy control (AKOSi009-a). Stem Cell Res [Internet] 2020;49:102079.vailable from: http://www.ncbi.nlm.nih.gov/pubmed/33197697
30. Peter F, Trilck M, Rabenstein M, Rolfs A, Frech MJ. Dataset in support of the generation of Niemann-pick disease type C1 patient-specific iPS cell lines carrying the novel NPC1 mutation c.1180T>C or the prevalent c.3182T>C mutation – analysis of pluripotency and neuronal differentiation. Data Br [Internet] 2017;12:123–131. Available from: http://www.ncbi.nlm.nih.gov/pubmed/28413817
31. Zanon A, Kalvakuri S, Rakovic A, Foco L, Guida M, Schwienbacher C, et al. SLP-2 interacts with parkin in mitochondria and prevents mitochondrial dysfunction in parkin-deficient human iPSC-derived neurons and drosophila. Hum Mol Genet [Internet] 2017;26(13):2412–2425. Available from: https://academic.oup.com/hmg/article/26/13/2412/3098491
32. Trilck-Winkler M, Borsche M, König IR, Balck A, Lenz I, Kasten M, et al. Parkin deficiency appears not to Be associated with cardiac damage in Parkinson's disease. Mov Disord [Internet] 2021;36(1):271–273. Available from: https://onlinelibrary.wiley.com/doi/10.1002/mds.28422
33. Baud A, Wessely F, Mazzacuva F, McCormick J, Camuzeaux S, Heywood WE, et al. Multiplex high-throughput targeted proteomic assay to identify induced pluripotent stem cells. Anal Chem [Internet] 2017;89(4):2440–2448. Available from: https://pubs.acs.org/doi/10.1021/acs.analchem.6b04368
34. Reinhardt P, Glatza M, Hemmer K, Tsytsyura Y, Thiel CS, Höing S, et al. Derivation and expansion using only small molecules of human neural progenitors for neurodegenerative disease modeling. PLoS One [Internet] 2013;8(3):e59252. Available from: http://www.ncbi.nlm.nih.gov/pubmed/23533608
35. Berenguer-Escuder C, Grossmann D, Antony P, Arena G, Wasner K, Massart F, et al. Impaired mitochondrial-endoplasmic reticulum interaction and mitophagy in Miro1-mutant neurons in Parkinson's disease. Hum Mol Genet [Internet] 2020;29(8):1353–1364. Available from: https://academic.oup.com/hmg/advance-article/doi/10.1093/hmg/ddaa066/5816586
36. Moltedo O, Remondelli P, Amodio G. The mitochondria–endoplasmic reticulum contacts and their critical role in aging and age-associated diseases. Front Cell Dev Biol [Internet] 2019;7:172. Available from: https://www.frontiersin.org/article/10.3389/fcell.2019.00172/full
37. Kornmann B, Osman C, Walter P. The conserved GTPase Gem1 regulates endoplasmic reticulum-mitochondria connections. Proc Natl Acad Sci [Internet] 2011;108(34):14151–14156. Available from: http://www.pnas.org/cgi/doi/10.1073/pnas.1111314108
38. Lee S, Lee K-S, Huh S, Liu S, Lee D-Y, Hong SH, et al. Polo kinase phosphorylates Miro to control ER-mitochondria contact sites and mitochondrial Ca 2+ homeostasis in neural stem cell development. Dev Cell [Internet] 2016 Apr;37(2):174–189. Available from:. https://doi.org/10.1016/j.devcel.2016.03.023
39. Berenguer-Escuder C, Grossmann D, Massart F, Antony P, Burbulla LF, Glaab E, et al. Variants in Miro1 cause alterations of ER-mitochondria contact sites in fibroblasts from Parkinson's disease patients. J Clin Med [Internet] 2019;8(12):2226. Available from: http://www.ncbi.nlm.nih.gov/pubmed/31888276
40. Nemani N, Carvalho E, Tomar D, Dong Z, Ketschek A, Breves SL, et al. MIRO-1 determines mitochondrial shape transition upon GPCR activation and Ca2+stress. Cell Rep 2018;23(4):1005–1019.
41. Hajnóczky G, Booth D, Csordás G, Debattisti V, Golenár T, Naghdi S, et al. Reliance of ER–mitochondrial calcium signaling on mitochondrial EF-hand Ca2+ binding proteins: Miros, MICUs, LETM1 and solute carriers. Curr Opin Cell Biol [Internet] 2014;

29(1):133–141. Available from: http://linkinghub.elsevier.com/retrieve/pii/S0955067414000738

42. Lytton J, Westlin M, Hanley MR. Thapsigargin inhibits the sarcoplasmic or endoplasmic reticulum Ca-ATPase family of calcium pumps. J Biol Chem [Internet] 1991;266(26):17067–17071. Available from: http://www.ncbi.nlm.nih.gov/pubmed/1832668

43. Eiyama A, Okamoto K. PINK1/parkin-mediated mitophagy in mammalian cells. Curr Opin Cell Biol [Internet] 2015 Apr;33:95–101. Available from: http://www.ncbi.nlm.nih.gov/pubmed/25697963

44. Barazzuol L, Giamogante F, Brini M, Calì T. PINK1/parkin mediated mitophagy, Ca2+ Signalling, and ER-mitochondria contacts in Parkinson's disease. Int J Mol Sci [Internet] 2020;21(5):1772. Available from: http://www.ncbi.nlm.nih.gov/pubmed/32150829

45. Bravo R, Vicencio JM, Parra V, Troncoso R, Munoz JP, Bui M, et al. Increased ER–mitochondrial coupling promotes mitochondrial respiration and bioenergetics during early phases of ER stress. J Cell Sci [Internet] 2011;124(13):2143–2152. Available from: https://journals.biologists.com/jcs/article/124/13/2143/31830/Increased-ER-mitochondrial-coupling-promotes

46. Saotome M, Safiulina D, Szabadkai G, Das S, Fransson A, Aspenstrom P, et al. Bidirectional Ca2+−dependent control of mitochondrial dynamics by the Miro GTPase. Proc Natl Acad Sci [Internet] 2008;105(52):20728–20733. Available from: http://www.pnas.org/cgi/doi/10.1073/pnas.0808953105

47. Niescier RF, Hong K, Park D, Min K-T. MCU interacts with Miro1 to modulate mitochondrial functions in neurons. J Neurosci [Internet] 2018;38(20):4666–4677. Available from: http://www.ncbi.nlm.nih.gov/pubmed/29686046

48. Jackson JG, Robinson MB. Reciprocal regulation of mitochondrial dynamics and calcium signaling in astrocyte processes. J Neurosci [Internet] 2015;35(45):15199–15213. Available from: http://www.jneurosci.org/cgi/doi/10.1523/JNEUROSCI.2049-15.2015

49. Treiman M, Caspersen C, Christensen SB. A tool coming of age: thapsigargin as an inhibitor of sarco-endoplasmic reticulum Ca(2+)-ATPases. Trends Pharmacol Sci [Internet] 1998;19(4):131–135. Available from: http://www.ncbi.nlm.nih.gov/pubmed/9612087

50. Guardia-Laguarta C, Liu Y, Lauritzen KH, Erdjument-Bromage H, Martin B, Swayne TC, et al. PINK1 content in mitochondria is regulated by ER-associated degradation. J Neurosci [Internet] 2019;39(36):7074–7085. Available from: http://www.jneurosci.org/lookup/doi/10.1523/JNEUROSCI.1691-18.2019

51. Trychta KA, Bäck S, Henderson MJ, Harvey BK. KDEL receptors are differentially regulated to maintain the ER proteome under calcium deficiency. Cell Rep [Internet] 2018;25(7):1829–1840.e6. Available from: https://linkinghub.elsevier.com/retrieve/pii/S2211124718316449

Supporting Data

Additional Supporting Information may be found in the online version of this article at the publisher's web-site.